Making quantitative sense of electromicrobial production

Nico J. Claassens[†‡], Charles A.R. Cotton[†‡], Dennis Kopljar[‡‡], Arren Bar-Even[†*]

[†] Max Planck Institute of Molecular Plant Physiology, Am Mühlenberg 1, 14476 Potsdam-Golm, Germany

[‡] German Aerospace Center (DLR), Institute of Engineering Thermodynamics, Pfaffenwaldring 38-40, 70569 Stuttgart, Germany

[‡] These authors contributed equally to this study

* corresponding author; phone: +49 331 567-8910; Email: Bar-Even@mpimp-golm.mpg.de

Key words: microbial electrosynthesis; electrochemistry; renewable feedstocks; one carbon metabolism; lithotrophic growth; cost analysis

Abstract

The integration of electrochemical and microbial processes offers a unique opportunity to displace fossil carbon with CO_2 and renewable energy as the primary feedstocks for carbon-based chemicals. Yet, it is unclear which strategy for CO_2 activation and electron transfer to microbes has the capacity to transform the chemical industry. Here, we systematically survey experimental data for microbial growth on compounds that can be produced electrochemically, either directly or indirectly. We show that only a few strategies can support efficient electromicrobial production, where formate and methanol seem the best electron mediators in terms of energetic efficiency of feedstock bio-conversion under both anaerobic and aerobic conditions. We further show that direct attachment of microbes to the cathode is highly constrained due to an inherent discrepancy between the rates of the electrochemical and biological processes. Our quantitative perspective provides a data-driven roadmap towards economically and environmentally viable realization of electromicrobial production.

Introduction

Establishing a circular carbon economy is imperative for reducing carbon dioxide emissions and weaning industry from its dependence on fossil carbon. At its core, a circular carbon economy demands the use of CO_2 as the fundamental feedstock for the production of carbon-commodities. Production of chemicals and fuels based on photosynthetic carbon assimilation – by plants, algae or cyanobacteria – is unlikely to be a long-term solution due to inherent low efficiency[1–4], erosion of food security and biodiversity, and inefficient use of resources such as water and minerals[5]. On the other hand, non-biological catalytic conversion of CO_2 into complex chemicals is challenging due to low product selectivity, use of environmentally hazardous substances, and the requirement of high temperature and pressure[6,7]. An emerging solution, which has gained substantial momentum in the past decade, is to integrate physicochemical and biological processes to optimize CO_2 conversion into biomass and carbon commodities[8–10]. The capture of renewable energy – solar, wind, hydro, and geothermal – is most efficiently performed using non-biological means, such as photovoltaic cells, concentrated solar technologies, or wind and water turbines. Electricity, the key product of most of these energy conversion technologies, can then be used to energize microbial growth and CO_2 conversion into products of interests – a process that we refer to as electromicrobial production.

Electromicrobial production thus provides one of the most promising ways to realize the vision of a circular carbon economy[4,7,8]. A key challenge in this technology is the transfer of reducing power from the abiotic (electrodes) to the biotic (microbial) world. As shown in Figure 1A, this can be sustained via direct attachment of the microbes to the cathode (usually referred to as microbial electrosynthesis[8]) where electrons are either transferred directly to the microorganism or are used to generate a reduced compound that is consumed *in situ* by the attached microbe. Alternatively, electrons can be shuttled to the microorganism using a mediator compound that is consumed by free floating microbes as a growth feedstock. Such electron carriers include, for example, hydrogen[11–13], inorganic ions (e.g., ferrous ions, ammonia, nitrite, sulfide[14,15]), and simple organic molecules (e.g., carbon monoxide, formate, methanol, ethanol[11,16]). These compounds can be produced either directly via an electrochemical process (Figure 1B) or via a two-step process in which hydrogen, produced from water electrolysis, is catalytically reacted with CO_2 or another inorganic compound (Figure 1C).

Despite the substantial progress demonstrated with different electromicrobial production strategies, it remains unclear which holds real transformative potential. The purpose of this study is to systematically analyze and compare different electromicrobial production strategies. We compile a comprehensive dataset of experimentally measured microbial growth parameters and use it to calculate the energetic efficiency and electron consumption rate associated with the use of different electron mediators and pathways. We show that under both anaerobic and aerobic conditions, formate and methanol are the best mediators in terms of energetic efficiency. We further demonstrate – using both a back-of-the-envelope calculation and a simplified cost estimation model – that direct attachment of microbes to the electrode is highly limited by a low current density, favoring spatial decoupling of the electrochemical and biological processes. We combine these analyses with several other physicochemical considerations (e.g., insolubility of gaseous mediators) to highlight the advantages and disadvantages of different electromicrobial production strategies.

Results

Comprehensive analysis of microbial growth on electron carriers

We first analyzed microbial consumption of electron carriers (Figure 1B,C) by conducting a comprehensive literature search to collect measured growth rates and yields. Our survey included microbial growth on hydrogen and organic compounds that can potentially be produced via electrochemical reduction of CO_2: C1 compounds, including carbon monoxide, formate, methanol, and methane, and C2 compounds, including ethanol, acetate, and oxalate. We further considered inorganic electron carriers: ferrous ion, ammonia, nitrite, sulfide, thiosulfate, and phosphite. Complex organic electron shuttles, such as phenazines, flavins or methyl viologen[8], were not considered, as information on their uptake rates and conversion efficiencies is scarce.

Regarding terminal electron acceptors, only two molecules – oxygen and carbon dioxide – are freely available and hence are reasonable to use from a biotechnological perspective. Accordingly, we analyze growth using the reductive acetyl-CoA pathway, the only anaerobic route that can use CO_2 as sole electron acceptor; aerobic growth on C1 compounds (including H_2/CO_2); aerobic growth on C2 compounds; and aerobic growth on reduced inorganic compounds. Overall, we compiled a comprehensive database containing >200 entries of experimentally measured growth parameters sub-classified by assimilation pathways (**Supplementary Data 1**).

We use these experimental values to derive two key growth properties: energetic efficiency of substrate conversion and rate of electron consumption. As electricity generation has a significant environmental footprint and is an expensive input for electromicrobial production[17], the energetic efficiency of substrate conversion has a decisive effect on the sustainability and economics of the overall process. As explained in detail in the Methods, the energetic efficiency was calculated as the percentage of the combustion energy of the substrate that is retained in either the product (for anaerobic growth, inherently coupled to the biosynthesis of a specific compound) or in the biomass (for aerobic growth, in which byproducts are mostly absent). As a complementary factor, we normalized the feedstock consumption rate to represent the rate of electron consumption, enabling us to compare the productivity limit associated with different feedstocks (Methods). All values are given in the **Supplementary Data 1**. Figure 2 presents the characteristic energetic efficiencies and electron consumption rates of all electrons carriers and pathways analyzed.

We note that while energetic efficiency represents a rather fixed (pathway-dependent) thermodynamic-stoichiometric constraint, electron consumption rate might be more amenable to improvement, e.g., by fine tuning cellular metabolism or by lab evolution to increase feedstock uptake rate. As such, energetic efficiency presents a more stringent criterion for evaluating the suitability of feedstocks and pathways to support electromicrobial production.

Anaerobic growth via the reductive acetyl-CoA pathway

Our analysis shows that (anaerobic) acetogens display high energetic efficiency of substrate to product conversion, characteristically 70-90% (Figure 2). The reductive acetyl-CoA pathway, used by acetogens, is the only metabolic route that provides energy to the cell (in the form of ATP) while assimilating and reducing CO_2 and/or C1 compounds[18]. To generate ATP for cellular growth and maintenance, the cell metabolizes (most of)

the C1 electron carrier into a secreted product. Since the energy gain from this conversion is low, the vast majority of the electrons in the feedstock are channeled towards the product to generate a sufficient amount of cellular energy, resulting in a high product yield and energetic efficiency[18]. As shown in Figure 2, acetogenic growth also supports a high electron consumption rate which can reach 100 µmol-electrons per second per gram dry cell weight (gDCW).

Interestingly, the energetic efficiency associated with growth of acetogens on the rarely used feedstocks formate and methanol is higher than that achieved with the more commonly used hydrogen. On the other hand, growth on the higher energy substrate carbon monoxide lowers the product yield and hence the energetic efficiency. This seemingly counterintuitive observation stems from the fact that more ATP molecules can be produced per consumed substrate, freeing more substrate molecules to be used for biomass generation rather than energy conservation via product biosynthesis.

Despite several advantages, bioproduction using acetogens has distinctive drawbacks. While recently developed genetic tools enable the establishment of new biosynthesis routes in acetogens[19,20], the product spectrum of these microorganisms remains limited. One of the main reasons for this is energetic limitation: only compounds whose biosynthesis generates ATP can be produced. As a result, acetogenic production is constrained to chemicals such as ethanol, isopropanol, n-butanol, and 2,3-butanediol[21,22]. Only acetate and ethanol are currently produced by acetogens without byproducts. Moreover, despite high electron consumption rate, the overall productivity of acetogens is limited by two factors: (i) low growth rate, characteristically < 0.05 h^{-1}; and (ii) low maximal cell concentration[23], characteristically < 5 $g \cdot L^{-1}$, which is an order of magnitude lower than aerobic microbes[24,25].

Methanogens also use the reductive acetyl-CoA pathway for anaerobic growth. In general, the energetic efficiencies and electron consumption rates associated with methanogens are similar to those of acetogens (not shown in Figure 2, see **Supplementary Data 1**). Methanogenic growth on hydrogen under thermophilic conditions uniquely displays an impressive electron consumption rate, up to 500 µmol-electrons per second per gDCW (**Supplementary Data 1**). Yet, while genetic tools for engineering methanogens are becoming available[26,27], using methanogens to produce compounds other than methane is highly challenging.

Only few promising feedstocks and metabolic pathways for aerobic growth

In aerobic growth, bioproduction and cellular energy conservation are largely decoupled, thus removing the thermodynamic restrictions associated with anaerobic growth and allowing for the biosynthesis of any chemical of interest. The energetic efficiency obtained in aerobic feedstock conversion is however much lower than that reached anaerobically, as a substantial fraction of the feedstock electrons ends up reducing O_2 to water rather than in the product. As experimental data on aerobic product yields using C1 feedstocks are scarce, we instead used the widely available data for biomass yield. While product and biomass yields do not necessarily correlate (as the former strongly depends upon the chosen product and the biosynthesis route), biomass yield provides the only useful benchmark for comparison of different feedstocks and pathways. (Production yields from different C1 feedstocks are available only for polyhydroxybutyrate; the higher biomass yield of methylotrophic growth compared to autotrophic growth – as discussed below – is indeed reflected by a somewhat higher polyhydroxybutyrate yield, see **Supplementary Data 1**).

Figure 2 shows that the energetic efficiency of aerobic feedstock to biomass conversion strongly depends on the growth substrate and metabolic pathway. For C1/C2 substrates this energetic efficiency lies in the range of 20-55% (for comparison, it is 50-60% for aerobic growth on glucose, as shown in **Supplementary Data 1**). Autotrophic growth using inorganic electron carriers (other than hydrogen) is characterized by high electron consumption rates but low energetic efficiencies, 5-30% (a few thermophilic exceptions for thiosulfate consumption are shown in **Supplementary Data 1**). This low efficiency practically rules out inorganic electron carriers from supporting efficient electromicrobial production (with the possible exception of acetogenic phosphite utilization, as discussed below).

Autotrophic growth on H_2/CO_2 or C1 feedstocks – using the Calvin Cycle – requires large ATP investment which leads to a rather low energetic efficiency of 20-35%. The serine cycle[28,29] can support high energetic efficiency for formate assimilation, 35-55%, but only moderate efficiency for methanol assimilation, 30-40%; yet, the electron consumption rate for growth on methanol is generally higher than that on formate (Figure 2). The lower energetic efficiency associated with growth on methanol can be attributed to the use of a quinone-dependent methanol dehydrogenase (MDH): electron transfer from methanol to the high-reduction potential quinones dissipates a substantial fraction of the available energy in the feedstock.

The energetic efficiency associated with methanol assimilation via the RuMP cycle[29], i.e., 40-50%, is significantly higher than that of the serine cycle (Figure 2). This higher efficiency is expected due to the lower ATP requirement of the RuMP cycle and the use of NAD-dependent MDH which does not waste energy during methanol oxidation. The dihydroxyacetone cycle, operating in methylotrophic yeasts, supports an intermediate efficiency of methanol assimilation, 30-40%. Methanotrophs operate at a relatively low energetic efficiency, 20-30%, regardless of the route they are using for formaldehyde assimilation (i.e., serine cycle or RuMP cycle). This is to be expected, as methane is oxidized to methanol wastefully using O_2 as oxidant and at the additional expense of NAD(P)H, such that half the reducing power in the feedstock is effectively dissipated[30]. Amongst the C2 feedstocks, ethanol and acetate support high energetic efficiency of 35-55%, while growth on oxalate – via, e.g., the glycerate pathway[31] or serine cycle[32] – results in a lower efficiency of 25-30%.

Overall, our analysis illustrates that only four feedstock-pathway combinations support aerobic energetic efficiency higher than 40%: formate assimilation via the serine cycle, methanol assimilation via the RuMP cycle, ethanol assimilation, and acetate assimilation. Amongst the C1 feedstocks, methanol assimilation via RuMP cycle has an advantage over formate assimilation via the serine cycle due to a higher electron consumption rate.

Direct attachment of microbes to the cathode limits current density

Direct attachment of microbes to the cathode, such that electrons are transferred either via a physical connection or via a short distance mediator (e.g., H_2, Figure 1A), has previously been discussed as the primary mode of electromicrobial production[8,33]. The main advantage of this approach is its very high energetic efficiency, up to 90% for the conversion of electricity to product[33]. However, microbial attachment to the cathode suffers from a number of drawbacks. First, it is limited to a small group of organisms – mostly anaerobic microbes which use the reductive acetyl-CoA pathway – hence resulting in a restricted product spectrum (mostly acetate and methane)[33]. Second, optimizing conditions for the activity of the electrochemical

and biochemical processes together – in terms of temperature, pH, electrolyte composition, etc. – is challenging[34] and is unlikely to reach the maximal potential of the two systems when run independently.

One might argue that these issues could be resolved by extensive engineering. Yet, there is one major drawback that would be very difficult to resolve, as it stems from basic physical-biochemical limits: the very low current density microbial-cathode attachment systems are able to support. While electrochemical production of electron carriers such as H_2, carbon monoxide, or formate can operate at hundreds of $mA \cdot cm^{-2}$ [35], current densities demonstrated for cathodic microbial attachment are mostly in the range of 1-10 $mA \cdot cm^{-2}$.[33]

A simple back-of-the-envelope calculation shows that this constraint would be almost impossible to overcome. Even if we assume a very thick metabolically active biofilm of 100 µm[36–38] (neglecting the non-metabolically active intercellular matrix[39]), we reach only ~0.005 gDCW per cm^2 of electrode surface area (characteristic density of bacteria is 0.5 $gDCW \cdot cm^{-3}$).[40] Using this estimate, a high electron consumption rate of 100 µmol-electrons per second per gDCW (Figure 2) gives a maximal current density of only ~50 $mA \cdot cm^{-2}$. The highest current density demonstrated for direct microbial-cathode attachment – using a 3D porous electrode – is 17.5 $mA \cdot cm^{-2}$,[41] still below this limit. This current density is at least an order of magnitude lower than the state-of-the-art for the electrochemical production of hydrogen[42,43], carbon monoxide[35,44,45], and formate[46,47]. This serves to emphasize the disparity between the rates of the electrochemical system and the biochemical system, highlighting the potential value of spatial decoupling of the two processes.

Economic interplay between energetic efficiency and current density

Following the observations described above, we aimed to compare the relative contribution of energetic efficiency and current density to the cost of the electrochemical process. When considering the economics of electrosynthesis it is a common practice to focus mainly on the cost of electricity, which is considered to be the most expensive feedstock[17,48]. This emphasizes the importance of energetic efficiency but fails to fully capture the costs associated with the size of the electrochemical reactor, i.e. of the electrolyzer, which is mostly determined by the current density. Depending on the system and its operating conditions, the contribution of the electrolyzer size to the overall cost can be substantial and even exceed the cost of electricity. To illustrate this quantitatively, we developed a simplified cost model for the electrochemical generation of electron carriers, enabling us to compare the relative effect of energetic efficiency and current density on the production cost (Methods).

In contrary to electrochemical water splitting (water electrolysis), electrochemical reduction of CO_2 is still at a relatively early stage of development and commercial applications have not yet been demonstrated. Therefore, we base our analysis on the mature technology of alkaline water electrolysis (AEL), which has been comprehensively explored and for which reliable techno-economic data exists[49,50]. This technology can be adapted for CO_2 reduction with minor adjustments (gaseous supply of reactant and different cathode architecture, **Supplementary Figure 1**), while maintaining the same cost structure[35,43,51]. Importantly, AEL enables the use of a liquid electrolyte that is well suited both for microbial attachment to the cathode and for the production of electron carriers. For the sake of comparison, we also analyzed the main competing technology: polymer electrolyte membrane electrolysis (PEMEL). While PEMEL is generally less suitable for electromicrobial production – as it uses highly acidic Nafion-ionomer and is associated with costly membrane-

electrode-assembly, precious metal catalysts, and manufacturing of the bipolar plate[52] – it can follow a varying input voltage more quickly, a marked advantage when using intermittent renewable electricity.

To derive a general expression of the production cost, we express it per unit of charge (€·kAh^{-1}), which directly relates to the number of electrons transferred to generate the desired product (1 kAh = 37.4 moles of electrons). The total cost of electrolysis is comprised of the investment and operation costs associated with the electrolyzer stack, which scales with the current density, and of the cost of electricity, which scales with the energetic efficiency. All assumptions, input parameters, and calculations are described in the Method section and in **Supplementary Table 1**.

Figure 3A shows the electrolysis cost C_{total} obtained from our model as a function of energetic efficiency and current density. The monotonically increasing thick black line represents combinations of EE and i in which electricity cost and stack-related costs (investment and operational costs) are equal. The area above a line is dominated by electricity cost and area below a line is dominated by the stack cost. The dashed lines represent deviations from the base case scenario towards one or more boundary values, as explained in the Methods. The light blue light corresponds to the PEMEL technology (Methods). Figure 3B corresponds to boundary combinations where the ratio between the stack-related cost and the cost of electricity is the highest and lowest.

It is clear from Figure 3 that regardless of the specific electrolysis product and exact input parameters, working at a low current density (≤10 mA·cm^{-2}, typical for microbial attachment to an electrode) translates into substantial stack size that would be highly costly, even if the energetic efficiency is close to 100%. At this range, C_{total} is always dominated by the cost of the stack while increased efficiency has a negligible effect on the overall cost. On the other hand, working at a high current density of hundreds of mA·cm^{-2} (typical for electrochemical production of hydrogen, carbon monoxide, and formate) results in a lower C_{total} than the former case, even at low energetic efficiencies. This analysis thus suggests that the high current density achieved with the production of electron carriers translates into lower electrolysis costs than with microbial attachment to the cathode despite the high energetic efficiency associated with the latter. Our findings illustrates that decoupling the electrochemical and biological processes is advantageous also from an economic point of view.

Direct and indirect electrochemical production of electron carriers

Direct electrochemical production of electron carriers (Figure 1B) is currently viable for only three compounds – hydrogen, carbon monoxide, and formate. These can be produced electrochemically with energetic efficiency ≥ 40%, Faraday efficiency ≥ 80%, and current density ≥ 300 mA·cm^{-2}.[35,53,54] This is not surprising, as the production of these compounds involves the transfer of a single pair of electrons. In contrast, the direct electrochemical synthesis of other C1/C2 molecules, which depends on multiple electron transfer steps – such as methanol, methane, ethylene, acetate, and ethanol – is generally characterized by a low energetic efficiency, Faraday efficiency, and/or current density[35,55].

Catalytic hydrogenation provides an alternative to direct electrochemical production (Figure 1C). Specifically, electrochemically produced hydrogen can be reacted with CO_2 in well-established catalytic processes to generate carbon monoxide (reverse water gas shift), methane (methanation), or methanol. These processes

are more mature than electrochemical production of carbon monoxide or formate and, despite requiring high temperature and pressure, can support high energetic efficiencies (Figure 4). For example, production of methane[56,57] and methanol[58,59] using this approach can already reach an overall energetic efficiency higher than 50%, surpassing even 70% using emerging technologies[60–62]. Despite the early stage, hydrogenation of CO_2 to formate has gained considerable attention in recent years and may prove an effective approach[63,64]. Hydrogen, produced electrochemically, can also be used in the well-established Haber-Bosch process to produce the electron carrier ammonia; the overall energetic efficiency of this process, from electricity to product, is also above 50%[65,66].

The high efficiency by which many electron carriers can be produced from hydrogen may cast doubt on the usefulness of direct electrochemical production of these compounds. However, hydrogenation processes require very large facilities and high investment. The electrochemical process, on the other hand, is more flexible and requires fewer catalytic steps. Importantly, the electrochemical process can also be ramped up and down, while catalytic hydrogenation is very challenging to operate under dynamic reaction conditions[67] which would be imposed by the intermittent nature of renewable electricity sources. Hence, when possible, a direct, flexible electrochemical route is likely to be preferable over a multi-step, large-volume, and non-dynamic hydrogenation-dependent production process.

Physicochemical considerations regarding different electron carriers

The physicochemical properties of the electron carriers further affect their suitability to support electromicrobial production. Unlike methanol and formate that are completely miscible, the low solubility of H_2 and CO – Henry's constants of 7.8 x 10^{-4} M·atm^{-1} and 9.7 x 10^{-4} M·atm^{-1}, as compared to 3.4 x 10^{-2} M·atm^{-1} for CO_2[68] – limits their mass transfer to the microbial culture, which is known to constrain productivity and require costly apparatus[23]. While methane is more soluble (Henry's constants of 1.4 x 10^{-3} M·atm^{-1}), its mass transfer still limits bio-consumption. The explosiveness of hydrogen and methane and the toxicity of carbon monoxide further require dedicated safety measures that increase costs. Moreover, as the retention time of gases within a liquid medium is short, they need to be continuously recycled, which costs energy and requires dedicated machinery.

A related constraint is the low solubility of O_2, which is required for aerobic bioproduction. It is well known that oxygen transfer rate can limit aerobic processes, requiring specialized bioreactor designs[69,70]. Yet, as the Henry's constant of O_2 (1.3 x 10^{-3} M·atm^{-1}) is higher than that of H_2 and CO, its solubility is less restricting than that of the reduced gases. Aeration also does not require considerable safety measures and does not need costly gas recycling. On the other hand, consumption of oxygen during aerobic processes generates a lot of heat and requires cooling systems to avoid deleterious increase of the temperature within the bioreactor[69].

Despite having several concrete advantages, the use of soluble electron carriers creates problems that are less common with the gaseous carriers. One of these relates to that fact that the soluble carriers are usually added to the culture in a diluted rather than pure form. While the purification of methanol and formate from water – an energetically expensive process[71] – is not required, the concentration of these electron carriers in the feedstock solution should be high enough as to avoid substantial dilution of the culture that would limit titer and productivity. Moreover, transfer of electrolytes from the electrolyzer into the microbial feedstock could

inhibit cellular growth[16,34], and might require costly recycling of the salts. To minimize this problem, electrolytes should be limited to benign salts and their concentrations should be minimized as much as possible, without severely reducing the conductivity necessary for the operation of the electrolyzer.

Formate presents another challenge. This compound can be produced either under neutral or alkaline conditions, giving rise to a formate salt (e.g., HCOOK), or under acidic conditions (pH < 3.5), where formic acid (pKa = 3.75) is the main product. Bio-consumption of formic acid is preferred as it is a proton neutral process, while the consumption of formate ions generates OH^- which requires the addition of an acid (e.g., HCl) to balance the pH, thus leading to the deleterious accumulation of salt (e.g., KCl). While the vast majority of studies have used neutral to alkaline conditions for electrochemical generation of formate, recently, the efficient production of a pure formic acid solution (without electrolytes) was demonstrated[72], thus potentially supporting a proton-balanced bio-consumption of this C1 carrier.

Another problem associated with methanol and formate is cellular toxicity. The toxicity of methanol relates mostly to its oxidation to the reactive intermediate formaldehyde[73] (hence, acetogenic consumption of methanol, which bypasses formaldehyde generation[74], is advantageous). Formate toxicity is attributed to inhibition of respiratory cytochromes[75] and to dissipation of the proton motive force by the diffusion of the protonated acid across the cell membrane[76]. Working with formic acid, rather than formate, can further decrease the pH and inhibit growth. Due to these issues, the concentration of methanol and formate must remain relatively low – few % (v/v) for methanol[77,78] and few grams per liter for formate[79,80] – making batch bioproduction impractical. Fed-batch cultivation is also challenging, as the addition of diluted feedstock would increase the culture volume quickly. This leaves continuous cultivation as the preferred option, where a constant inflow of concentrated methanol/formate/formic acid is balanced with outflow of culture medium, keeping a constant, low concentration of the electron carrier within the bioreactor.

Discussion

The comprehensive analysis performed in this study leads to several conclusions, mainly with regards to strategies that are less likely to be viable. First, attachment of microbes to an electrode is severely limited by low current densities, which is expected to substantially increase costs, making the economic feasibility of this approach problematic. Also, as the energetic efficiency associated with the aerobic oxidation of inorganic electron carriers is very low, the use of these mediator molecules is unlikely to provide a practical strategy. Moreover, the use of C2 feedstocks seems challenging due to either low efficiency of biological conversion (oxalate) or low efficiency of electrochemical/catalytic production (acetate and ethanol).

This leaves the use of C1 compounds, including H_2/CO_2, as the most promising approach for electromicrobial production. Yet, there is no clear champion when it comes to the exact identity of the C1 electron carrier or the bioproduction conditions. As summarized in Figure 5, each choice comes with its own advantages and disadvantages. Aerobic conditions, while restricted in energetic efficiency and limited by the solubility of O_2, can support the bioproduction of a wide array of compounds, including chemicals whose biosynthesis consumes, rather than produces, ATP. Under these conditions, only growth on formate via the serine cycle or growth on methanol via the RuMP cycle seems to support reasonably high energetic efficiency. Yet, the toxicity of these electron carriers might require specialized process design.

Anaerobic production can support unrivalled energetic efficiencies but has a limited product spectrum. Hydrogen and carbon monoxide are by far the most commonly used feedstocks for acetogenic growth, but their low solubility constrains mass transfer and the safety measures they require increase costs. While CO generally supports a lower yield than H_2, its higher energy content enables the efficient production of otherwise difficult to synthesize reduced compounds – for example, ethanol[81]. Cultivation of acetogens on formate or methanol – potentially supporting an even higher energetic efficiency – provides a thus far unexplored alternative strategy that can alleviate mass transfer limitations.

An interesting option is the use of multiple electron carriers in parallel, which could boost the energetic efficiency and widen the product spectrum. A recent study demonstrated the strength of this approach by electrochemically producing syngas – a combination of H_2 and CO – at almost 100% Faraday efficiency and a current density of 300 $mA \cdot cm^{-2}$. The syngas was subsequently fed to a co-culture of two *Clostridia* strains (including an acetogen), leading to a conversion of electricity into butanol and hexane at a very high overall energetic efficiency of 78%.[11]

Some electromicrobial production systems are not yet available, but could offer considerable advantages if established. For example, engineering microorganisms for growth on C1-compounds via novel assimilation routes – e.g., the synthetic reductive glycine pathway which was designed to be the most efficient route for aerobic formate assimilation[82,83] – could enable model biotechnological organisms, such as *E. coli*, to support highly efficient electromicrobial production[84]. Alternatively, novel electrochemical strategies might enable direct CO_2 reduction to acetate or ethanol at sufficiently high energetic efficiency, Faraday efficiency, and current density, thus paving the way for a C2-dependent electromicrobial production. Establishing efficient electro-recycling of phosphate into the low reduction-potential phosphite would provide another interesting electromicrobial production setup, as anaerobic growth of acetogens on phosphite is highly efficient[85].

Finally, either the abiotic process or the biotic process could be split into two parts, the combination of which allows for high performance that is difficult to obtain without such division. We discussed above how a two-step catalytic process can efficiently produce compounds whose direct electrochemical synthesis is inefficient, e.g., methanol. From a biological perspective, acetogenic growth on H_2/CO/formate under anaerobic conditions can be coupled with subsequent aerobic microbial growth on acetate, for the production of a wide scope of chemicals, as demonstrated by several studies[86–88]. As many biotechnological model microbes can natively grow on acetate, coupling acetate bioproduction with its bio-consumption could prove to be a useful electromicrobial production approach. The energetic efficiency of such a multi-step process could be quite high: 70% for electrochemical production of H_2, 75% for acetogenic consumption of hydrogen (Figure 2), and 50% for acetotrophic bioproduction (Figure 2), translates to an overall ~26% energetic efficiency from electricity to a product. The downside of splitting a process into two segments is the need for more reactors and intermediate steps (e.g., separation) which might increase production cost.

The challenges limiting the expansion of renewable energy and sustainable production of chemicals require an immediate response. We hope that the analysis we provide in this study will serve as a roadmap for sustainable and economically feasible realization of electromicrobial production.

Figure Legends

Figure 1

A schematic representation of the three main types of electromicrobial production. (A) Direct attachment of the microbes to the cathode, which is usually referred to as microbial electrosynthesis. Electrons are either transferred directly to the microbes or are used to generate a compound (e.g., CO) that is consumed *in situ*. (B) Direct electrochemical production: electron carrier (e.g., CO) is produced at the cathode and then transferred and introduced to free floating microbes, either in the same reactor or a separate one. (C) Catalytic hydrogenation (indirect electrochemical production): hydrogen is generated at the cathode and then reacted, in a separate catalytic process, with CO_2 to generate an electron carrier (e.g., CO) which is subsequently fed to a microbial reactor.

Figure 2

Microbial growth parameters associated with different feedstocks and assimilation pathways. Rectangles represent the 25-75% percentile values and the crosses correspond to the standard errors ($\sigma/\sqrt{n}$) around the mean values, as calculated using experimentally measured values for mesophilic microorganisms (see **Supplementary Data 1** for complete set of values for all microorganisms, which also includes information on thermophilic growth; our data suggest that the parameters of mesophilic and thermophilic growth are in the same range, the only exceptions being methanogenic growth on hydrogen and aerobic growth on thiosulfate). Data for methanogens are available in **Supplementary Data 1**, and are generally comparable to those for acetogens. Energetic efficiency was calculated as the fraction of the combustion energy of the substrate that is retained in the product (for acetogens) or biomass (for aerobic microbes). Rate of electron consumption was either derived from the consumption rate of the feedstock (if reported) or calculated from the growth yield and growth rates. Detailed explanation of the calculations is provided in the Methods and the calculations are presented in **Supplementary Data 1**.

Figure 3

Approximated costs of electro-production of electron carriers as a function of energetic efficiency and current density. (A) Contour lines correspond to the base case assuming an electricity price $C_{electricity}$ of 0.05 €·kWh^{-1}, standard cell voltage U^o of 1.23 V (corresponding to electrochemical production of H_2), electrolyzer stack investment cost of 580 €·kW^{-1}, and Faraday Efficiency of 90%. The monotonically increasing black line represents combinations of energetic efficiency and current density in which the cost of the electrolyzer stack and the cost of electricity are equal. Accordingly, the area above the line is dominated by electricity cost and area below the line is dominated by the stack cost. Dashed lines represent combinations of energetic efficiency and current density for which stack cost and electricity cost are equal for different boundary scenarios; in which U^o was taken as either 1 V or 1.5 V (corresponding to the range of U^o of all relevant C1 and C2 molecules with anodic oxygen evolution), $C_{electricity}$ was taken as either €0.03 kWh^{-1} or €0.07 kWh^{-1}, and the stack investment cost was taken as either €800 kW^{-1} or €370 kW^{-1} (boundary values of the projected cost range given in[50], see Methods). The light blue line corresponds to the PEMEL technology (Methods). Brown and purple areas correspond to the characteristic ranges of electromicrobial production via

a mediating electron carrier or via direct electron transfer from the cathode to attached microbes. (B) Total cost at the boundary combinations, where the ratio between the stack-related cost and the cost of electricity is the highest and lowest, respectively: (i) U^o = 1 V, C_{elec} = €0.03 kWh^{-1}, stack = €800 kW^{-1}; and (ii) U^o= 1.5 V, C_{elec} = €0.07 kWh^{-1}, stack = €370 kW^{-1}.

Figure 4

A two-step catalytic process can replace direct electrochemical production. Various compounds can be obtained from the reaction of CO_2 with electrochemically produced hydrogen. Numbers in blue boxes relate to the energetic efficiencies sustained by more mature technologies, while numbers in green boxes corresponds to efficiencies supported by emerging, less mature technologies. The initial step in these processes is hydrogen production via electrolysis, which already reaches an energetic efficiency of 70-80%[54]. Emerging high-temperature water electrolysis technologies can support efficiencies even higher than 85%[54,89–91]. Power-to-gas technologies enable the production of methane from electricity with an overall energetic efficiency of ~55%[57,58]. Heat integration or coupling with high-temperature electrolysis can further increase this efficiency to well above 70%[60–62]. Similarly, production of methanol from electricity can already reach an energetic efficiency higher than 50%[58,59]. Due to the early stage of the technology, no information on energetic efficiency of hydrogenation of CO_2 to produce formate is currently available. The overall energetic efficiency of ammonia production from electricity is also above 50%[65,66]; emerging technologies for direct electrochemical reduction of N_2 to ammonia which might be able to support efficiencies higher than 70%[65,66].

Figure 5

Summarized comparison between different C1 electron carriers. Shades of green and red represent how much the advantages and disadvantages hold true for the specific electron carriers. FE corresponds to Faraday efficiency, EE to energetic efficiency, CD to current density in mA/cm^2, K_H to Henry's constant, and NA to non-applicable.

Methods

Calculation of microbial energetic efficiency and electron consumption rate

Energetic efficiency was calculated as the percentage of the combustion energy of the substrate that is retained in either the product (for anaerobic growth) or in the biomass (for aerobic growth). Anaerobic growth (with CO_2 as an electron acceptor) is inherently coupled to the biosynthesis of a specific compound (e.g., acetate) while biomass formation is relatively low. Hence, in this case, we consider the energetic efficiency of converting feedstock into product, as calculated from experimentally measured product yields and the known combustion energies of feedstocks and products. That is:

Eq. 1 $$E_{anaer} = Y_{prod} \times {\Delta G_{comb}^{prod}}/{\Delta G_{comb}^{sub}}$$

where E_{anaer} is the efficiency of anaerobic conversion, Y_{prod} is the measured product yield (mole product per mole substrate), ΔG_{comb}^{prod} is the combustion energy of the product (kJ·mol^{-1}) and ΔG_{comb}^{sub} is the combustion energy of the substrate (kJ·mol^{-1}).

For aerobic growth, in which byproducts are mostly absent, we report the energetic efficiency of converting feedstock into biomass, as calculated from experimentally measured biomass yield and using the combustion energy of microbial biomass[92]. That is:

Eq.2 $$E_{aer} = Y_{biomass} \times {\Delta G_{comb}^{biomass}}/{\Delta G_{comb}^{sub}}$$

where E_{aer} is the efficiency of anaerobic conversion, $Y_{biomass}$ is the measured biomass yield (gram dry cell weight per mole substrate), $\Delta G_{comb}^{biomass}$ is the combustion energy of the product (20 kJ per gram dry cell weight[92]) and ΔG_{comb}^{sub} is the combustion energy of the substrate (kJ·mol^{-1}). While microbial biomass is rarely a desirable product by itself (with few exceptions[93]), we use biomass yield instead of product yield as information on the latter is scarce and the two yields are expected to correlate.

As a complementary factor, we normalized the feedstock consumption rate to represent the rate of electron consumption, enabling us to compare the productivity limit associated with feedstocks of different redox state. Thus, $V_e = V_f \times n_e^f$, where V_e is the electron consumption rate (μmol per second per gram dry cell weight), V_f is the experimentally measured feedstock consumption rate (same units), and n_e^f is the amount of available electrons in the feedstock, e.g., two for formate and six for methanol. If V_f was not reported, it was calculated from the measured growth yield and growth rates, such that $V_e = {\mu}/{Y_{prod}} \times n_e^f$, where μ is the growth rate (sec^{-1}) and Y_{prod} is the product yield, as defined above. See **Supplementary Data 1** for all calculations.

Cost analysis for electrochemical production

We developed a model for the cost of electrochemical production of H_2, C1 and C2 compounds which includes investment and operating costs for an electrolyzer stack as well as the cost of electricity. This model was intended to reveal the interplay between key factors that shape the economic competitiveness of

electrosynthesis, and, particularly, to identify the relative effect of current density and energetic efficiency on the overall cost. The model should be regarded as an attempt to uncover qualitative and general trends inherent to electrosynthesis rather than to deliver a sophisticated techno-economic analysis of production cost. By developing such a general model, we naturally neglect factors that contribute to the overall process economics, *e.g.* use of different catalysts and electrode structures to obtain different products. Yet, the sensitivity analysis we perform – with regards to the standard voltage, electricity price, and the cost of the electrolyzer stack – shows that the trends we find are general enough and do not change fundamentally with the exact choice of input parameters.

Only a few techno-economic models of electrochemical CO_2 reduction (CO2RR) have been published[35,51,94,95]. As no commercially available CO_2 electrolyzer (CO2EL) system exists, these models are based on the cost structure of and available information for water electrolysis. This is also the approach we followed. To predict the economics of CO2RR, we focused on state-of-the-art alkaline water electrolysis (AEL). This is because AEL uses a liquid electrolyte which can be adjusted in composition to facilitate microbial growth, supporting both attachment of microbes to the cathode and the electrochemical production of electron carriers. Furthermore, CO2RR has mostly been demonstrated in neutral to alkaline conditions thus supressing hydrogen evolution (HER, reduction of the aqueous electrolyte, the main side reaction in CO2RR) which is favoured at low pH. This makes the Membrane-Electrode-Assembly (MEA) approach, used in polymer-electrolyte membrane electrolysis (PEMEL) with the acidic Nafion-ionomer, less suitable for CO_2 reduction and for coupling of electrochemistry with microbial growth[96]. Yet, as PEMEL has the advantage of quickly responding to the fluctuating availability of renewable electricity, thus allowing a highly flexible operation, we decided to model it as well. A sketch of both setups is shown in **Supplementary Figure 1**.

Relevant reactions for hydrogen evolution and CO2RR, producing C1 and C2 compounds, are shown below for alkaline conditions (except for formic acid given in acidic conditions and HER in both) together with the standard cell voltage, U^0_{cell}, as determined by thermodynamics, assuming oxygen evolution at the anode[97].

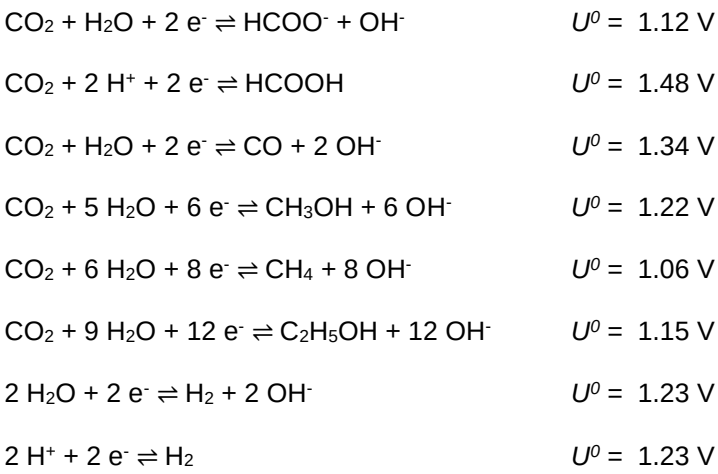

The main difference between AEL and CO2EL is the electrode architecture of the cathode side and the supply of reactant. A cost breakdown of the different contributions to the total stack cost assumes a cathode share of around 25% in alkaline water electrolysis[49], in which nickel-based electrodes are commonly employed. To account for the more costly manufacturing of the gas diffusion electrode (used in CO2EL to circumvent limited

CO_2 solubility and to facilitate the use of high current densities[43,46,98]), the additional gas feed, and other unique properties of the stack, a sensitivity analysis on the stack cost was performed, as explained below.

Supplementary Table 1 shows the values we used for the base case scenario for AEL, the boundary cases for AEL, and for PEMEL. Below, we explain each of these.

Stack investment cost

The investment cost is based on literature data of projected cost for water electrolysis systems in 2030. We used the data from the Fuel Cells and Hydrogen Joint Undertaking (FCH JU) which estimated the cost, in 2030, to range between €370 kW^{-1} and €800 kW^{-1} for AEL[50]. These values were used for the boundary scenarios, where the average value of €580 kW^{-1} was taken for the base case scenario. The investment cost for PEMEL was taken as €780 kW^{-1}.[50]

The investment cost comprises the entire uninstalled electrolyzer system, including the stack, power supply and electronics, and the periphery of the facility. The latter part, termed balance of plant (BOP), involves feed preparation, gas conditioning, thermal management, pumps and compression, and measurement and control technologies. We decided to focus only on the cost of the stack – which accounts for 50% and 60% of the investment cost in AEL and PEMEL, respectively[50] – as it is the only component that is directly equivalent between water to CO_2 electrolysis regardless of the exact configuration. Other components might change according to the specific application and the subsequent processing (*e.g.*, H_2 storage vs. production of liquid products or subsequent microbial upgrading). Accordingly, the periphery cost for CO2RR and their scaling with electrolyzer size (especially electrode area) is largely unknown.

Conversion from cost per nominal power to cost per electrode area

To express the investment cost associated with the stack as a function of the current density, the stack nominal power needs to be converted into an electrode area. That is, the cost that is usually given in €·kW^{-1} needs to be translated in €·m^{-2}. As reasonable approximation, the stack cost scales linearly with electrode size, as economy of scale is not pronounced for electrolyzer stacks[42]. To normalize for electrode area, the relationship between the nominal power *P* of a typical state-of-the-art water electrolyzer and the electrode area *A* is required. While the nominal power is given for commercial electrolyzer systems by the manufacturer, the electrode area can be estimated from the operating current density *i* and the total product yield $\dot{n}_{H2}$ (in mol·h^{-1}, equivalent to $\dot{V}_{H2,}/\, v_{mol}$, with $\dot{V}_{H2,}$ being the H_2 production rate in $Nm^3 \cdot h^{-1}$ and v_{mol} the molar volume) that relate to each other by Faraday's Law according to:

Eq. 3
$$\dot{n}_{H2} = \frac{I}{z \cdot F} FE = \frac{i \cdot A}{z \cdot F} FE$$

with *z* being the number of transferred electrons per turnover, *F* the Faraday constant and *FE* the Faraday efficiency (share of charge going into the desired product, ~1 for water electrolysis). Rearranging eq. 3, the estimated electrode area can be calculated by:

Eq. 4
$$A_{electrode} = \frac{\dot{V}_{H2,out} \cdot z \cdot F}{v_{mol} \cdot i}$$

A similar calculation relating area and power was done by Jouney et al.[35], but only for one exemplary alkaline electrolyzer. To account for the different operating conditions and stack properties of different technologies and manufacturers, and to put our input parameters on a solid basis, our data is based on the comprehensive market survey of Buttler and Spliethoff from 2017[42]. Using the reported hydrogen production rates, the corresponding nominal power, and a typical current density of 300-400 mA·cm^{-2} for AEL and 1-2 A·cm^{-2} for PEMEL, we obtained an average factor of 7 kW·m^{-2} (5-8 kW·m^{-2}) between power and estimated electrode area for the reported 15 commercial alkaline electrolyzer systems and 32 kW·m^{-2} for the 8 PEMEL systems. Including an installation factor of 10% (a typical value for electrolysis[42], but which could easily be higher given the high complexity of the presented technology), an average investment cost of ~€2,300 m^{-2} for AEL can be obtained. This value is very close to the one obtained by Li et al.[95] for alkaline CO2EL (€1221-4884 m^{-2}, base case of €2442 m^{-2}), supporting the validity of our assumptions and approach. With the same approach, PEMEL stack cost amounts to ~€16,000 m^{-2} which is significantly higher due to the expensive materials used (catalyst, membrane, bipolar plates).

In the next step, the cost per area is converted into cost per charge (€·kAh^{-1}) by dividing by the current density and by *FE*, the latter accounting for charge that goes into side products. Applying Faraday's Law which correlates charge to the amount of product, this could further be translated into the cost per product yield, if desired.

To distribute the cost over the run time of the electrolyzer, a simple financial model was implemented, assuming fixed payment at equal intervals. Using an interest rate *r* of 5% on the capital investment and a loan term of 20 years[51], the annual cost can be calculated as fixed-rate mortgage[99] according to:

Eq. 5
$$C_{year} = C_0 \frac{(1+r)^{years} \cdot r}{(1+r)^{years} - 1}$$

We assume an average annual run time of 5000 hours/year at nominal capacity as to account for the limited availability of cheap renewable electricity and to enable process flexibility according to the volatile electricity market[54].

Non-electricity related operating cost

The operating cost can be divided into an electricity-dependent part and a maintenance part. The latter is required to keep the electrolyzer running and is commonly given as percentage on the initial investment cost and includes replacement of electrode and electrocatalyst, as well as electrolyte replenishment and general maintenance of the system. This cost ranges between 2 and 5% of the initial (uninstalled) investment cost per year, depending on the size of the electrolyzer, with smaller systems having higher maintenance cost[50]. As CO_2 electrolysis is not as mature as water electrolysis and long-term stability of electrode materials has yet to be demonstrated, we chose a value of 5%. (Even a higher value might be well justified, in view of the high complexity of the technology. This would result in higher stack-related cost and further strengthen our argument.) The cost or credit associated with the use of CO_2 and water are not included as these are difficult to estimate. We emphasize again that we did not perform a thorough simulation on material and energy fluxes as this would go beyond the scope of this contribution and would not comply with our approach to derive a general model for cost analysis.

Electricity cost

For the electricity cost we use a value of €0.05 kWh^{-1}, following reported wholesale electricity prices in 2018[100]. For the sensitivity analysis we used boundary cases of €0.03 kWh^{-1} and €0.07 kWh^{-1}. To obtain the electricity cost normalized on the charge, i.e., €·kAh^{-1}, the price per kWh was divided by the operating cell voltage (as energy = voltage · charge) and by FE to account for the charge that went into the production of side products. The energetic efficiency (*EE*) is defined as:

Eq. 6 $$EE = \frac{U^0}{U_{cell}} FE$$

where the actual cell voltage U_{cell} is a function of *EE* and the standard cell voltage U^0 of the overall reaction – cathode plus anode - the latter represents oxygen evolution. As a base case, water electrolysis was chosen with U^0 = 1.23 V (E^0 = 0 V for hydrogen evolution). To cover the standard voltages for all relevant C1 and C2 products from above, we used 1 V to 1.5 V as boundary cases.

Total cost

Finally, the total cost, in in €·kAh^{-1}, is given by:

Eq. 7 $$C_{total} = \frac{C_{stack}+C_{operation}}{i \cdot FE} + C_{electricity} \cdot \frac{U^0}{EE}$$

where C_{stack} is the depreciated investment cost associated with the electrolyzer stack (in units of €·m^{-2}·h^{-1}, see below), $C_{operation}$ is the operating cost excluding electricity (normalized on electrode area, €·m^{-2}·h^{-1}), $C_{electricity}$ is the cost of electricity (€·kWh^{-1}) and the other parameters are as mentioned.

Sensitivity analysis

To avoid the model being biased by the choice of input parameters, we performed a sensitivity analysis in which the investment cost, standard cell voltage (characteristic for the targeted product) and electricity price were varied according to the boundary values mentioned above. Specifically, for the investment cost we used €370 kW^{-1} and €800 kW^{-1} as boundary values according to the range projected for 2030 (see above), for the cell voltage we used 1 V to 1.5 V which accounts for production of all targeted C1 and C2 products, and for electricity cost we used €0.03 kWh^{-1} and €0.07 kWh^{-1}, which represent a deviation of 40% of the base value. Accordingly, at the extreme are scenarios in which the ratio between stack-related cost and electricity cost is the highest (scenario 1: €800 kW^{-1} investment cost, 1 V standard cell voltage, €0.03 kWh^{-1} electricity cost) and a scenario in which this ration is the lowest (scenario 2: €370 kW^{-1}, 1.5 V, €0.07 kWh^{-1}). In scenario 1, the influence of current density is most pronounced over energetic efficiency, while in scenario 2 it is the reverse.

As a final note, we would like to emphasize that the maintenance cost and installation factor were chosen conservatively – in the sense that they reduce the overall contribution of the current density – and could easily be higher than assumed, further increasing investment cost and, thus, the influence of current density.

Acknowledgements

The authors thank Ron Milo, Simon Geiger, Aldo Gago, Avi Flamholz, Hai He, Dirk Holtmann, Frank Kensy, Elad Noor, and Ari Satanowski for helpful discussions and critical reading of the manuscript. This work received funding from the Max Planck Society and from the European Union's Horizon 2020 research and innovation programme under grant agreement No. 763911 (Project eForFuel). N.J.C. is supported by The Netherlands Organization for Scientific Research (NWO) through a Rubicon Grant (Project 019.163LW.035).

Author contributions

A.B.-E. conceptualized and supervised the research; N.J.C., C.A.R.C., and A.B.-E. designed and performed the quantitative microbial analysis; D.K. performed the electrolysis cost analysis; N.J.C., C.A.R.C., D.K., and A.B.-E. analyzed the data and wrote the paper.

Competing interests statement

A.B.-E. is cofounder of b.fab, exploring the commercialization of microbial bioproduction using formate as feedstock. The company was not involved in any way in performing or funding this study.

ORCID

Nico J. Claassens: 0000-0003-1593-0377

Charles A. R. Cotton: 0000-0002-5322-5292

Dennis Kopljar: 0000-0002-2228-2016

Arren Bar-Even: 0000-0002-1039-4328

Data availability

The data that support the plots within this paper and other findings of this study are available from the corresponding author upon reasonable request.

Supplementary information

Supplementary Data 1 presents the growth parameters collected from the literature and the calculated energetic efficiencies and electron consumption rates.

Supplementary Table 1 presents the assumption taken for the cost analysis of electrosynthesis.

Supplementary Figure 1 shows schemes of the electrolysis technologies considered in this study.

References

1. Zhu, X.-G., Long, S. P. & Ort, D. R. What is the maximum efficiency with which photosynthesis can convert solar energy into biomass? *Curr. Opin. Biotechnol.* **19,** 153–159 (2008).
2. Cotton, C. A. R. *et al.* Photosynthetic constraints on fuel from microbes. *Front. Bioeng. Biotechnol.* **3,** 1–5 (2015).
3. Blankenship, R. E. *et al.* Comparing photosynthetic and photovoltaic efficiencies and recognizing the potential for improvement. *Science* **332,** 805–809 (2011).
4. Claassens, N. J., Sousa, D. Z., Dos Santos, V. A. P. M., De Vos, W. M. & Van Der Oost, J. Harnessing the power of microbial autotrophy. *Nat. Rev. Microbiol.* **14,** 692–706 (2016).
5. Naik, S. N., Goud, V. V., Rout, P. K. & Dalai, A. K. Production of first and second generation biofuels: A comprehensive review. *Renew. Sustain. Energy Rev.* **14,** 578–597 (2010).
6. Conrado, R. J. & Gonzalez, R. Envisioning the bioconversion of methane to liquid fuels. *Science* **343,** 621–623 (2014).
7. Liao, J. C., Mi, L., Pontrelli, S. & Luo, S. Fuelling the future: microbial engineering for the production of sustainable biofuels. *Nat. Rev. Microbiol.* **14,** 288–304 (2016).
8. Rabaey, K. & Rozendal, R. A. Microbial electrosynthesis - revisiting the electrical route for microbial production. *Nat. Rev. Microbiol.* **8,** 706–716 (2010).
9. Liu, C. *et al.* Nanowire–Bacteria Hybrids for Unassisted Solar Carbon Dioxide Fixation to Value-Added Chemicals. *Nano Lett.* **15,** 3634–3639 (2015).
10. Conrado, R. J., Haynes, C. A., Haendler, B. E. & Toone, E. J. Electrofuels: A New Paradigm for Renewable Fuels. in *Advanced Biofuels and Bioproducts* 1037–1064 (Spinger, 2013).
11. Haas, T., Krause, R., Weber, R., Demler, M. & Schmid, G. Technical photosynthesis involving CO_2 electrolysis and fermentation. *Nat. Catal.* **1,** 32–39 (2018).
12. Torella, J. P. *et al.* Efficient solar-to-fuels production from a hybrid microbial–water-splitting catalyst system. *Proc. Natl. Acad. Sci. U.S.A.* **112,** 2337–2342 (2015).
13. Liu, C. *et al.* Water splitting-biosynthetic system with CO_2 reduction efficiencies exceeding photosynthesis. *Science* **352,** 1210–1213 (2016).
14. Khunjar, W. O., Sahin, A., West, A. C., Chandran, K. & Banta, S. Biomass Production from Electricity Using Ammonia as an Electron Carrier in a Reverse Microbial Fuel Cell. *PLoS One* **7,** 1–8 (2012).
15. Guan, J. *et al.* Development of reactor configurations for an electrofuels platform utilizing genetically modified iron oxidizing bacteria for the reduction of CO_2 to biochemicals. *J. Biotechnol.* **245,** 21–27 (2017).
16. Li, H. *et al.* Integrated Electromicrobial Conversion of CO_2 to Higher Alcohols. *Science* **335,** 1596–1596 (2012).
17. Khan, N. E., Myers, J. A., Tuerk, A. L. & Curtis, W. R. A process economic assessment of hydrocarbon biofuels production using chemoautotrophic organisms. *Bioresour. Technol.* **172,** 201–211 (2014).
18. Schuchmann, K. & Müller, V. Autotrophy at the thermodynamic limit of life: a model for energy conservation in acetogenic bacteria. *Nat. Rev. Microbiol.* **12,** 809–821 (2014).
19. Charubin, K., Bennett, R. K., Fast, A. G. & Papoutsakis, E. T. Engineering Clostridium organisms as microbial cell-factories: challenges & opportunities. *Metab. Eng.* **50,** 173–191 (2018).
20. Schiel-Bengelsdorf, B. & Dürre, P. Pathway engineering and synthetic biology using acetogens. *FEBS Lett.* **586,** 2191–2198 (2012).
21. Humphreys, C. M. & Minton, N. P. Advances in metabolic engineering in the microbial production of fuels and chemicals from C1 gas. *Curr. Opin. Biotechnol.* **50,** 174–181 (2018).
22. Köpke, M. *et al.* 2,3-Butanediol production by acetogenic bacteria, an alternative route to chemical synthesis, using industrial waste gas. *Appl. Environ. Microbiol.* **77,** 5467–5475 (2011).
23. Abubackar, Haris Nalakath Veiga, M. C. & Kennes, C. Biological conversion of carbon monoxide: rich syngas or waste gases to bioethanol. *Biofuels, Bioprod. Biorefining* **5,** 93–114 (2011).
24. Knoll, A. *et al.* High cell density cultivation of recombinant yeasts and bacteria under non-pressurized and pressurized conditions in stirred tank bioreactors. *J. Biotechnol.* **132,** 167–179 (2007).
25. Garcia-Gonzalez, L., Mozumder, M. S. I., Dubreuil, M., Volcke, E. I. P. & De Wever, H. Sustainable autotrophic production of polyhydroxybutyrate (PHB) from CO_2 using a two-stage cultivation system. *Catal. Today* **257,** 237–245 (2015).
26. Lyu, Z. *et al.* Engineering the Autotroph Methanococcus maripaludis for Geraniol Production. *ACS Synth. Biol.* **5,** 577–581 (2016).
27. Nayak, D. D. & Metcalf, W. W. Cas9-mediated genome editing in the methanogenic archaeon Methanosarcina acetivorans. *Proc. Natl. Acad. Sci. U.S.A.* **114,** 2976–2981 (2017).
28. Anthony, C. *The biochemistry of methylotrophs*. (Academic Press, 1982).
29. Chistoserdova, L., Kalyuzhnaya, M. G. & Lidstrom, M. E. The Expanding World of Methylotrophic

Metabolism. *Annu. Rev. Microbiol.* **63,** 477–499 (2009).
30. Lawton, T. J. & Rosenzweig, A. C. Methane-Oxidizing Enzymes: An Upstream Problem in Biological Gas-to-Liquids Conversion. *J. Am. Chem. Soc.* **138,** 9327–9340 (2016).
31. Cornick, N. A. & Allison, M. J. Anabolic incorporation of oxalate by *Oxalobacter formigenes*. *Appl. Environ. Microbiol.* **62,** 3011–3013 (1996).
32. Schneider, K., Skovran, E. & Vorholt, J. A. Oxalyl-coenzyme A reduction to glyoxylate is the preferred route of oxalate assimilation in *Methylobacterium extorquens AM1*. *J. Bacteriol.* **194,** 3144–3155 (2012).
33. Tremblay, P. L. & Zhang, T. Electrifying microbes for the production of chemicals. *Front. Microbiol.* **6,** 1–10 (2015).
34. Sydow, A., Krieg, T., Ulber, R. & Holtmann, D. Growth medium and electrolyte - how to combine the different requirements on the reaction solution in bioelectrochemical systems using *Cupriavidus necator*. *Eng. Life Sci.* **17,** 781–791 (2017).
35. Jouny, M., Luc, W. W. W. & Jiao, F. A General Techno-Economic Analysis of CO₂ Electrolysis Systems. *Ind. Eng. Chem. Res.* **57,** (2018).
36. Cui, M., Nie, H., Zhang, T., Lovley, D. & Russell, T. P. Three-dimensional hierarchical metal oxide–carbon electrode materials for highly efficient microbial electrosynthesis. *Sustain. Energy Fuels* **1,** 1171–1176 (2017).
37. Aryal, N., Halder, A., Tremblay, P. L., Chi, Q. & Zhang, T. Enhanced microbial electrosynthesis with three-dimensional graphene functionalized cathodes fabricated via solvothermal synthesis. *Electrochim. Acta* **217,** 117–122 (2016).
38. Jourdin, L. & Strik, D. Electrodes for Cathodic Microbial Electrosynthesis Processes: Key Developments and Criteria for Effective Research and Implementation. in *Functional Electrodes for Enzymatic and Microbial Electrochemical Systems* 429–472 (World Scientific Publishing, 2017).
39. Flemming, H.-C., Wingender, J., Griebe, T. & Mayer, C. *Biofilms: Recent Advances in their Study and Control (Physicochemical properties of Biofilms)*. (Harwood academic publishers, 2000).
40. Loferer-Kroßbacher, M., Klima, J. & Psenner, R. Determination of Bacterial Cell Dry Mass by Transmission Electron Microscopy and Densitometric Image Analysis Downloaded from. *Appl. Envir. Microbiol.* **64,** 688–694 (1998).
41. Jourdin, L. *et al.* High Acetic Acid Production Rate Obtained by Microbial Electrosynthesis from Carbon Dioxide. *Environ. Sci. Technol.* **49,** 13566–13574 (2015).
42. Buttler, A. & Spliethoff, H. Current status of water electrolysis for energy storage, grid balancing and sector coupling via power-to-gas and power-to-liquids: A review. *Renew. Sustain. Energy Rev.* **82,** 2440–2454 (2018).
43. Martín, A. J. J., Larrazábal, G. O. O. & Pérez-Ramírez, J. Towards sustainable fuels and chemicals through the electrochemical reduction of CO_2: lessons from water electrolysis. *Green Chem.* **17,** 5114–5130 (2015).
44. Ma, S., Luo, R., Moniri, S., Lan, Y. & Kenis, P. J. A. Efficient Electrochemical Flow System with Improved Anode for the Conversion of CO_2 to CO. *J. Electrochem. Soc.* **161,** 1124–1131 (2014).
45. Jeanty, P. *et al.* Upscaling and continuous operation of electrochemical CO_2 to CO conversion in aqueous solutions on silver gas diffusion electrodes. *J. CO2 Util.* **24,** 454–462 (2018).
46. Kopljar, D., Inan, A., Vindayer, P., Wagner, N. & Klemm, E. Electrochemical reduction of CO_2 to formate at high current density using gas diffusion electrodes. *J. Appl. Electrochem.* **44,** 1107–1116 (2014).
47. Kopljar, D., Wagner, N. & Klemm, E. Transferring Electrochemical CO_2 Reduction from Semi-Batch into Continuous Operation Mode Using Gas Diffusion Electrodes. *Chem. Eng. Technol.* **39,** 2042–2050 (2016).
48. Harnisch, F., Rosa, L. F. M., Kracke, F., Virdis, B. & Kromer, J. O. Electrifying white biotechnology: Engineering and economic potential of electricity-driven bio-production. *ChemSusChem* **8,** 758–766 (2015).
49. Bertuccioli, L. *et al. Development of Water Electrolysis in the European Union*. (2014). Fuel Cells and Hydrogen Joint Undertaking. https://www.fch.europa.eu/sites/default/files/study electrolyser_0-Logos_0_0.pdf
50. *Commercialisation of Energy Storage in Europe: Final Report*. (2015). Fuel Cells and Hydrogen Joint Undertaking. https://www.fch.europa.eu/sites/default/files/CommercializationofEnergyStorageFinal_3.pdf
51. Verma, S., Kim, B., Jhong, H. R. M., Ma, S. & Kenis, P. J. A. A gross-margin model for defining technoeconomic benchmarks in the electroreduction of CO_2. *ChemSusChem* **9,** 1972–1979 (2016).
52. Schmidt, O. *et al.* Future cost and performance of water electrolysis: An expert elicitation study. *Int. J. Hydrogen Energy* **42,** 30470–30492 (2017).
53. Ainscough, C., Peterson, D. & Miller, E. *Hydrogen Production Cost From PEM Electrolysis*. (2014). US Department of Energy. https://www.hydrogen.energy.gov/pdfs/14004_h2_production_cost_pem_electrolysis.pdf

54. Bazzanella, A. M. & Ausfelder, F. *Low carbon energy and feedstock for the European chemical industry*. (2017). DECHEMA. https://dechema.de/dechema_media/Technology_study_Low_carbon_energy_and_feedstock_for_the_European_chemical_industry-p-20002750.pdf
55. Fan, Q. *et al.* Electrochemical CO_2 reduction to C2+ species: Heterogeneous electrocatalysts, reaction pathways, and optimization strategies. *Mater. Today Energy* **10,** 280–301 (2018).
56. Gotz, M. *et al.* Renewable Power-to-Gas : A technological and economic review. *Renew. Energy* **85,** 1371–1390 (2016).
57. Bailera, M., Lisbona, P., Romeo, L. M. & Espatolero, S. Power to Gas projects review: Lab, pilot and demo plants for storing renewable energy and CO_2. *Renew. Sustain. Energy Rev.* **69,** 292–312 (2017).
58. Mignard, D. & Pritchard, C. Processes for the synthesis of liquid fuels from CO_2 and marine energy. *Chem. Eng. Res. Des.* **84,** 828–836 (2006).
59. Szima, S. & Cormos, C. C. Improving methanol synthesis from carbon-free H_2 and captured CO_2: A techno-economic and environmental evaluation. *J. CO2 Util.* **24,** 555–563 (2018).
60. Kezibri, N. & Bouallou, C. Conceptual design and modelling of an industrial scale power to gas-oxy-combustion power plant. *Int. J. Hydrogen Energy* **42,** 19411–19419 (2017).
61. Gruber, M. *et al.* Power-to-Gas through thermal integration of high-temperature steam electrolysis and carbon dioxide methanation - Experimental results. *Fuel Process. Technol. J.* **181,** 61–74 (2018).
62. Salomone, F., Giglio, E., Ferrero, D., Santarelli, M. & Pirone, R. Techno-economic modelling of a Power-to-Gas system based on SOEC electrolysis and CO_2 methanation in a RES-based electric grid. *Chem. Eng. J.* (2018). doi:10.1016/j.cej.2018.10.170
63. Bulushev, D. A. & Ross, J. R. H. Heterogeneous catalysts for hydrogenation of CO_2 and bicarbonates to formic acid and formates. *Catal. Rev.* **60,** 566–593 (2018).
64. Alvarez, A. *et al.* Challenges in the Greener Production of Formates/Formic Acid, Methanol, and DME by Heterogeneously Catalyzed CO_2 Hydrogenation Processes. *Chem. Rev.* **117,** 9804–9838 (2017).
65. Wang, L. *et al.* Greening Ammonia toward the Solar Ammonia Refinery. *Joule* **2,** 1–20 (2018).
66. Jose Martin, A., Shinagawa, T. & Perez-Ramırez, J. Electrocatalytic Reduction of Nitrogen: From Haber-Bosch to Ammonia Artificial Leaf. *Chem* **5,** 1–21 (2019).
67. Kalz, K. F. *et al.* Future Challenges in Heterogeneous Catalysis: Understanding Catalysts under Dynamic Reaction Conditions. *ChemCatChem* **9,** 17–29 (2017).
68. Sander, R. Compilation of Henry's law constants (version 4.0) for water as solvent. *Atmos. Chem. Phys* **15,** 4399–4981 (2015).
69. Weusthuis, R. A., Lamot, I., van der Oost, J. & Sanders, J. P. M. C. N.-54. Microbial production of bulk chemicals: development of anaerobic processes. *Trends Biotechnol.* **29,** 153–158 (2011).
70. García-Ochoa, F. & Gómez, E. Bioreactor scale-up and oxygen transfer rate in microbial processes: an overview. *Biotechnol. Adv.* **27,** 153–76 (2009).
71. Greenblatt, J. B., Miller, D. J., Ager, J. W., Houle, F. A. & Sharp, I. D. The Technical and Energetic Challenges of Separating (Photo)Electrochemical Carbon Dioxide Reduction Products. *Joule* **2,** 381–420 (2018).
72. Yang, H., Kaczur, J. J., Sajjad, S. D. & Masel, R. I. CO_2 Conversion to Formic Acid in a Three Compartment Cell with Sustainion™ Membranes. *ECS Trans.* **77,** 1425–1431 (2017).
73. Pfeifenschneider, J., Brautaset, T. & Wendisch, V. F. Methanol as carbon substrate in the bio-economy: Metabolic engineering of aerobic methylotrophic bacteria for production of value-added chemicals. *Biofuels, Bioprod. Biorefining* **11,** 719–731 (2017).
74. Tremblay, P.-L., Höglund, D., Koza, A., Bonde, I. & Zhang, T. Adaptation of the autotrophic acetogen *Sporomusa ovata* to methanol accelerates the conversion of CO_2 to organic products. *Sci. Rep.* **5,** 16168 (2015).
75. Nicholls, P. Formate as an inhibitor of cytochrome c oxidase. *Biochem Biophys Res Commun.* **67,** 610–616 (1975).
76. Warnecke, T. & Gill, R. T. Organic acid toxicity, tolerance, and production in *Escherichia coli* biorefining applications. *Microb. Cell Fact.* **4,** 1–8 (2005).
77. Kim, P., Kim, J.-H. & Oh, D.-K. Improvement in cell yield of *Methylobacterium* sp. by reducing the inhibition of medium components for poly-β-hydroxybutyrate production. *World J. Microbiol. Biotechnol.* **19,** 357–361 (2003).
78. Choi, J.-H., Kim, J. H., Daniel, M. & Lebeault, J. M. Optimization of Growth Medium and Poly-hydroxybutyric Acid Production from Methanol in *Methylobacterium organophilum*. *Microbiol. Biotechnol. Lett.* **17,** 392–396 (1989).
79. Ahn, J. H., Bang, J., Kim, W. J. & Lee, S. Y. Formic acid as a secondary substrate for succinic acid production by metabolically engineered *Mannheimia succiniciproducens*. *Biotechnol. Bioeng.* **114,** 2837–2847 (2017).
80. Grunwald, S. *et al.* Kinetic and stoichiometric characterization of organoautotrophic growth of Ralstonia

eutropha on formic acid in fed-batch and continuous cultures. *Microb. Biotechnol.* **8,** 155–163 (2015).
81. Diender, M., Stams, A. J. M. & Sousa, D. Z. Pathways and Bioenergetics of Anaerobic Carbon Monoxide Fermentation. *Front. Microbiol.* **6,** 1–18 (2015).
82. Bar-Even, A., Noor, E., Flamholz, A. & Milo, R. Design and analysis of metabolic pathways supporting formatotrophic growth for electricity-dependent cultivation of microbes. *Biochim. Biophys. Acta* **1827,** 1039–47 (2013).
83. Bar-Even, A. Formate assimilation: The metabolic architecture of natural and synthetic pathways. *Biochemistry* **55,** 3851–3863 (2016).
84. Yishai, O., Bouzon, M., Döring, V. & Bar-Even, A. In vivo assimilation of one-carbon via a synthetic reductive glycine pathway in *Escherichia coli*. *ACS Synth. Biol.* **7,** 2023–2028 (2018).
85. Schink, B. & Friedrich, M. Phosphite oxidation by sulphate reduction. *Nature* **406,** 37 (2000).
86. Lehtinen, T. *et al.* Production of long chain alkyl esters from carbon dioxide and electricity by a two-stage bacterial process. *Bioresour. Technol.* **243,** 30–36 (2017).
87. Hu, P. *et al.* Integrated Bioprocess for Conversion of Gaseous Substrates to Liquids. *Proc. Natl. Acad. Sci. U.S.A.* **113,** 14–19 (2016).
88. Al Rowaihi, I. S. *et al.* A two-stage biological gas to liquid transfer process to convert carbon dioxide into bioplastic. *Bioresour. Technol. Reports* **1,** 61–68 (2018).
89. Posdziech, O. & Schwarze, K. Efficient hydrogen production for industry and electricity storage via high-temperature electrolysis. (2018). doi:10.1016/j.ijhydene.2018.05.169
90. Ebbesen, S. D., Jensen, S. H., Hauch, A. & Mogensen, M. B. High Temperature Electrolysis in Alkaline Cells , Solid Proton Conducting Cells , and Solid Oxide Cells. *Chem. Rev.* **114,** 10697–10734 (2014).
91. Patyk, A., Bachmann, T. M. & Brisse, A. Life cycle assessment of H_2 generation with high temperature electrolysis. *Int. J. Hydrogen Energy* **38,** 3865–3880 (2013).
92. Cordier, J. L., Butsch, B. M., Birou, B. & von Stockar, U. The relationship between elemental composition and heat of combustion of microbial biomass. *Appl. Microbiol. Biotechnol.* **25,** 305–312 (1987).
93. Pikaar, I. *et al.* Carbon emission avoidance and capture by producing in-reactor microbial biomass based food, feed and slow release fertilizer: Potentials and limitations. *Sci. Total Environ.* **644,** 1525–1530 (2018).
94. Spurgeon, J. M. & Kumar, B. A comparative technoeconomic analysis of pathways for commercial electrochemical CO_2 reduction to liquid products. *Energy Environ. Sci.* **11,** 1536–1551 (2018).
95. Li, X. *et al.* Greenhouse Gas Emissions, Energy Efficiency, and Cost of Synthetic Fuel Production Using Electrochemical CO_2 Conversion and the Fischer–Tropsch Process. *Energy & Fuels* **30,** 5980–5989 (2016).
96. Delacourt, C., Ridgway, P. L., Kerr, J. B. & Newman, J. Design of an Electrochemical Cell Making Syngas ($CO + H_2$) from CO_2 and H_2O Reduction at Room Temperature. *J. Electrochem. Soc.* **155,** B42–B49 (2008).
97. Bard, A., Parsons, R. & Jordan, J. *Standard potentials in aqueous solution*. (CRC Press, 1985).
98. Del Castillo, A. *et al.* Sn nanoparticles on gas diffusion electrodes: Synthesis, characterization and use for continuous CO_2 electroreduction to formate. *J. CO2 Util.* **18,** 222–228 (2017).
99. Schuster, T. & Rüdt von Collenberg, L. *Investitionsrechnung: Kapitalwert, Zinsfuß, Annuität, Amortisation*. (SpringerGabler, 2017).
100. *Quarterly report on European Electricity Markets*. *Market Observatory for Energy* **11,** (2018). European Commission. https://ec.europa.eu/energy/sites/ener/files/documents/quarterly_report_on_european_electricity_markets_q2_2018.pdf

Figure 1

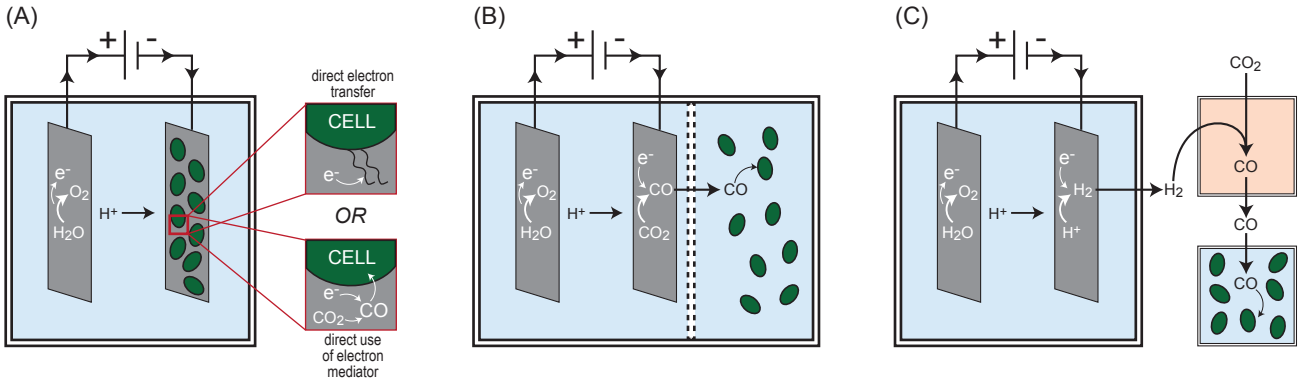
(A)
+
-
e⁻
O2
H2O
H+
direct electron transfer
CELL
e⁻
OR
CELL
e⁻
CO2
CO
direct use of electron mediator
(B)
+
-
e⁻
O2
H2O
H+
e⁻
CO
CO2
CO
(C)
+
-
e⁻
O2
H2O
H+
e⁻
H2
H+
H2
CO2
CO
CO
CO

Figure 2

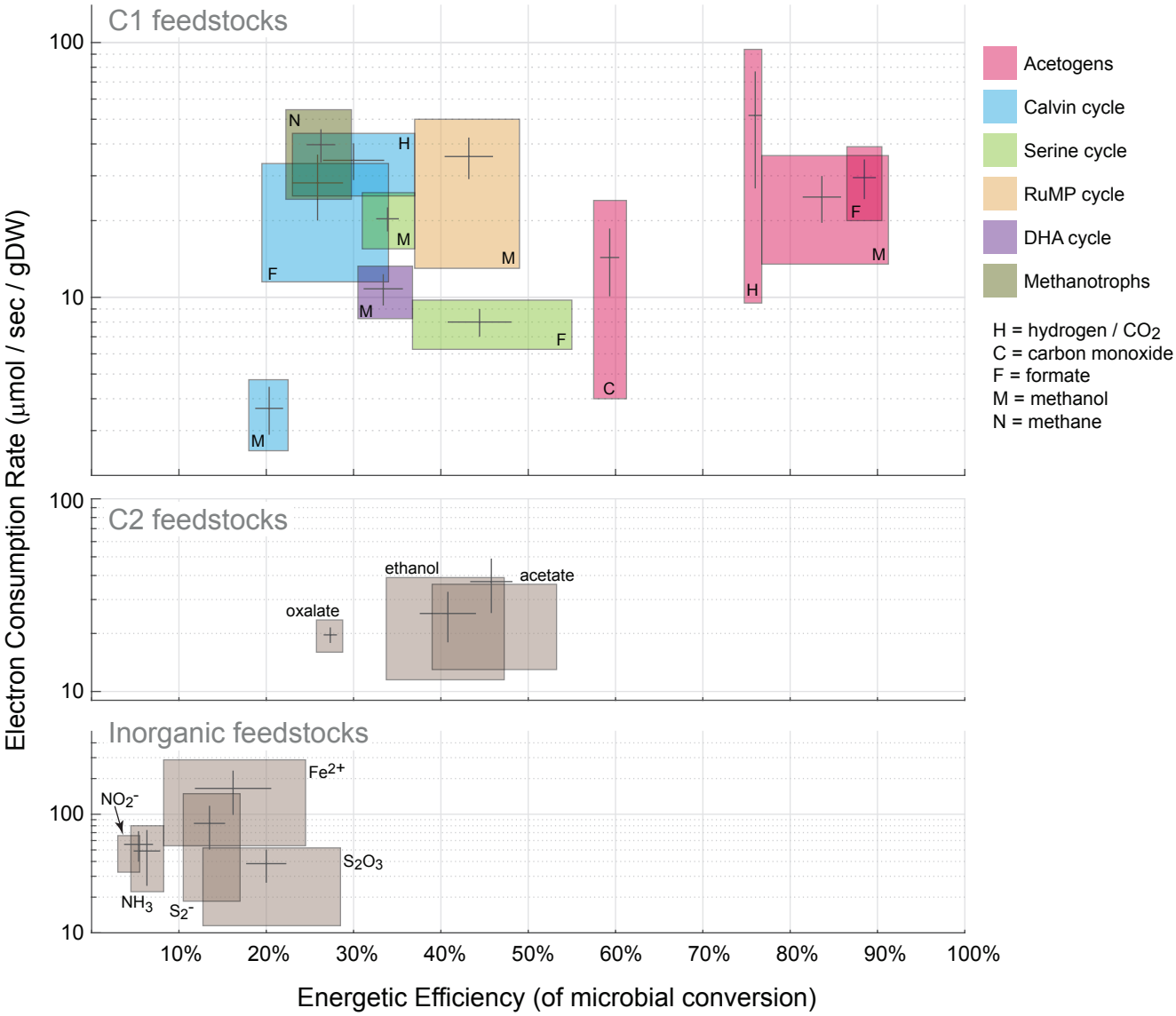
C1 feedstocks
C2 feedstocks
Inorganic feedstocks
Electron Consumption Rate (µmol / sec / gDW)
100
10
ethanol
acetate
oxalate
Fe^{2+}
NO_2^-
S_2O_3
NH_3
S_2^-
10%
20%
30%
40%
50%
60%
70%
80%
90%
100%
Energetic Efficiency (of microbial conversion)
Acetogens
Calvin cycle
Serine cycle
RuMP cycle
DHA cycle
Methanotrophs
H = hydrogen / CO_2
C = carbon monoxide
F = formate
M = methanol
N = methane

Figure 3

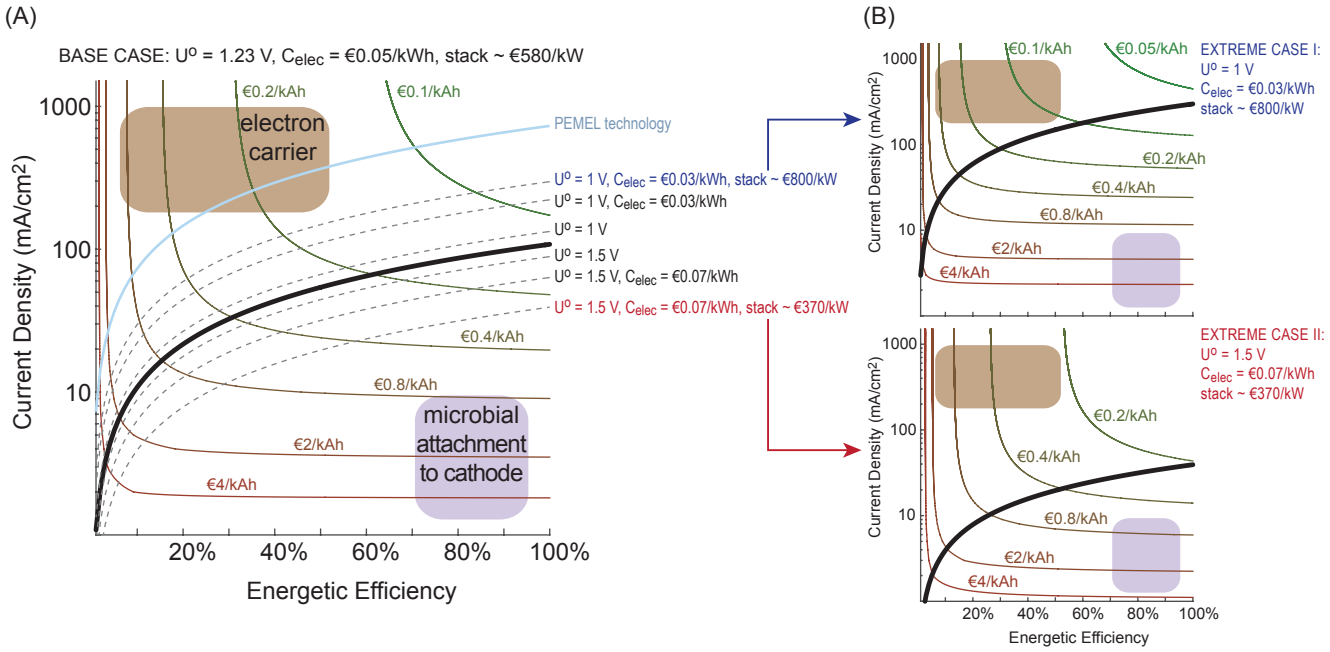
(A)
BASE CASE: U⁰ = 1.23 V, Celec = €0.05/kWh, stack ~ €580/kW
Current Density (mA/cm²)
1000
100
10
€0.2/kAh
€0.1/kAh
electron carrier
PEMEL technology
U⁰ = 1 V, Celec = €0.03/kWh, stack ~ €800/kW
U⁰ = 1 V, Celec = €0.03/kWh
U⁰ = 1 V
U⁰ = 1.5 V
U⁰ = 1.5 V, Celec = €0.07/kWh
U⁰ = 1.5 V, Celec = €0.07/kWh, stack ~ €370/kW
€0.4/kAh
€0.8/kAh
€2/kAh
€4/kAh
microbial attachment to cathode
20%
40%
60%
80%
100%
Energetic Efficiency
(B)
Current Density (mA/cm²)
1000
100
10
€0.1/kAh
€0.05/kAh
EXTREME CASE I:
U⁰ = 1 V
Celec = €0.03/kWh
stack ~ €800/kW
€0.2/kAh
€0.4/kAh
€0.8/kAh
€2/kAh
€4/kAh
EXTREME CASE II:
U⁰ = 1.5 V
Celec = €0.07/kWh
stack ~ €370/kW
20%
40%
60%
80%
100%
Energetic Efficiency

Figure 4

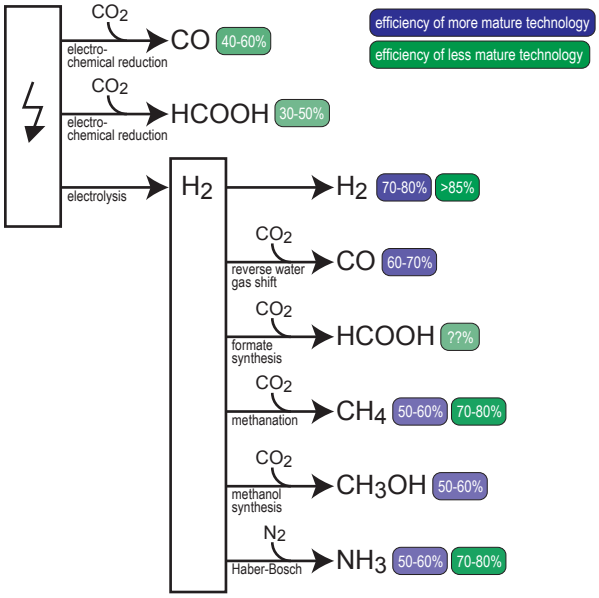
efficiency of more mature technology
efficiency of less mature technology
CO2
electro-
chemical reduction
CO
40-60%
CO2
electro-
chemical reduction
HCOOH
30-50%
electrolysis
H2
H2
70-80%
>85%
CO2
reverse water
gas shift
CO
60-70%
CO2
formate
synthesis
HCOOH
??%
CO2
methanation
CH4
50-60%
70-80%
CO2
methanol
synthesis
CH3OH
50-60%
N2
Haber-Bosch
NH3
50-60%
70-80%

Figure 5

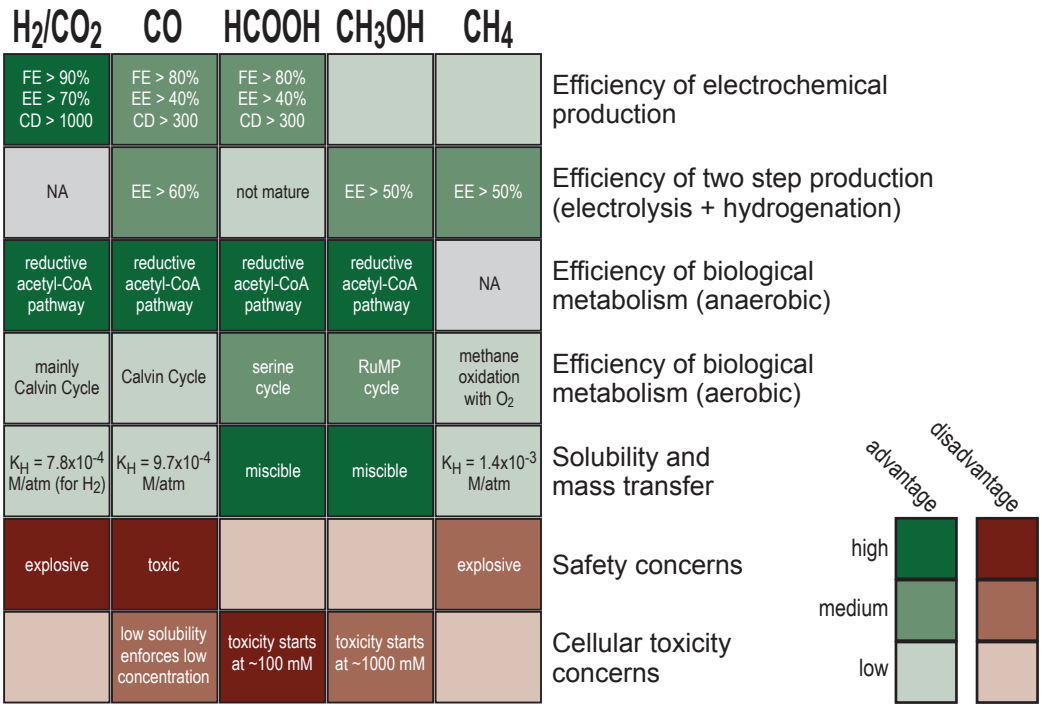
H_2/CO_2
CO
HCOOH
CH_3OH
CH_4
FE > 90% EE > 70% CD > 1000
FE > 80% EE > 40% CD > 300
FE > 80% EE > 40% CD > 300
NA
EE > 60%
not mature
EE > 50%
EE > 50%
reductive acetyl-CoA pathway
reductive acetyl-CoA pathway
reductive acetyl-CoA pathway
reductive acetyl-CoA pathway
NA
mainly Calvin Cycle
Calvin Cycle
serine cycle
RuMP cycle
methane oxidation with O_2
K_H = 7.8x10^{-4} M/atm (for H_2)
K_H = 9.7x10^{-4} M/atm
miscible
miscible
K_H = 1.4x10^{-3} M/atm
explosive
toxic
explosive
low solubility enforces low concentration
toxicity starts at ~100 mM
toxicity starts at ~1000 mM
Efficiency of electrochemical production
Efficiency of two step production (electrolysis + hydrogenation)
Efficiency of biological metabolism (anaerobic)
Efficiency of biological metabolism (aerobic)
Solubility and mass transfer
Safety concerns
Cellular toxicity concerns
advantage
disadvantage
high
medium
low

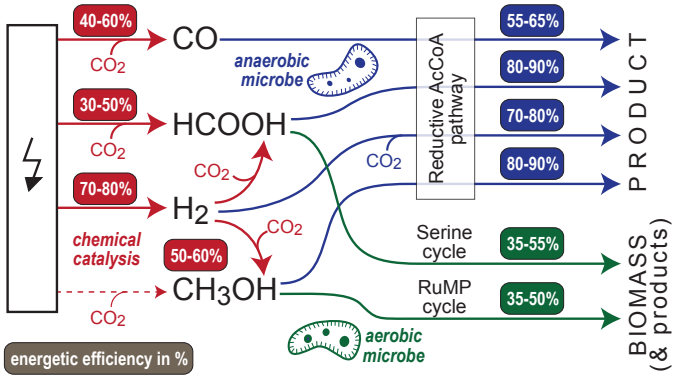
40-60%
CO
CO2
anaerobic microbe
30-50%
HCOOH
CO2
70-80%
H2
CO2
chemical catalysis
50-60%
CH3OH
CO2
energetic efficiency in %
Reductive AcCoA pathway
CO2
55-65%
80-90%
70-80%
80-90%
PRODUCT
Serine cycle
35-55%
RuMP cycle
35-50%
BIOMASS (& products)
aerobic microbe

Supplementary Figure 1

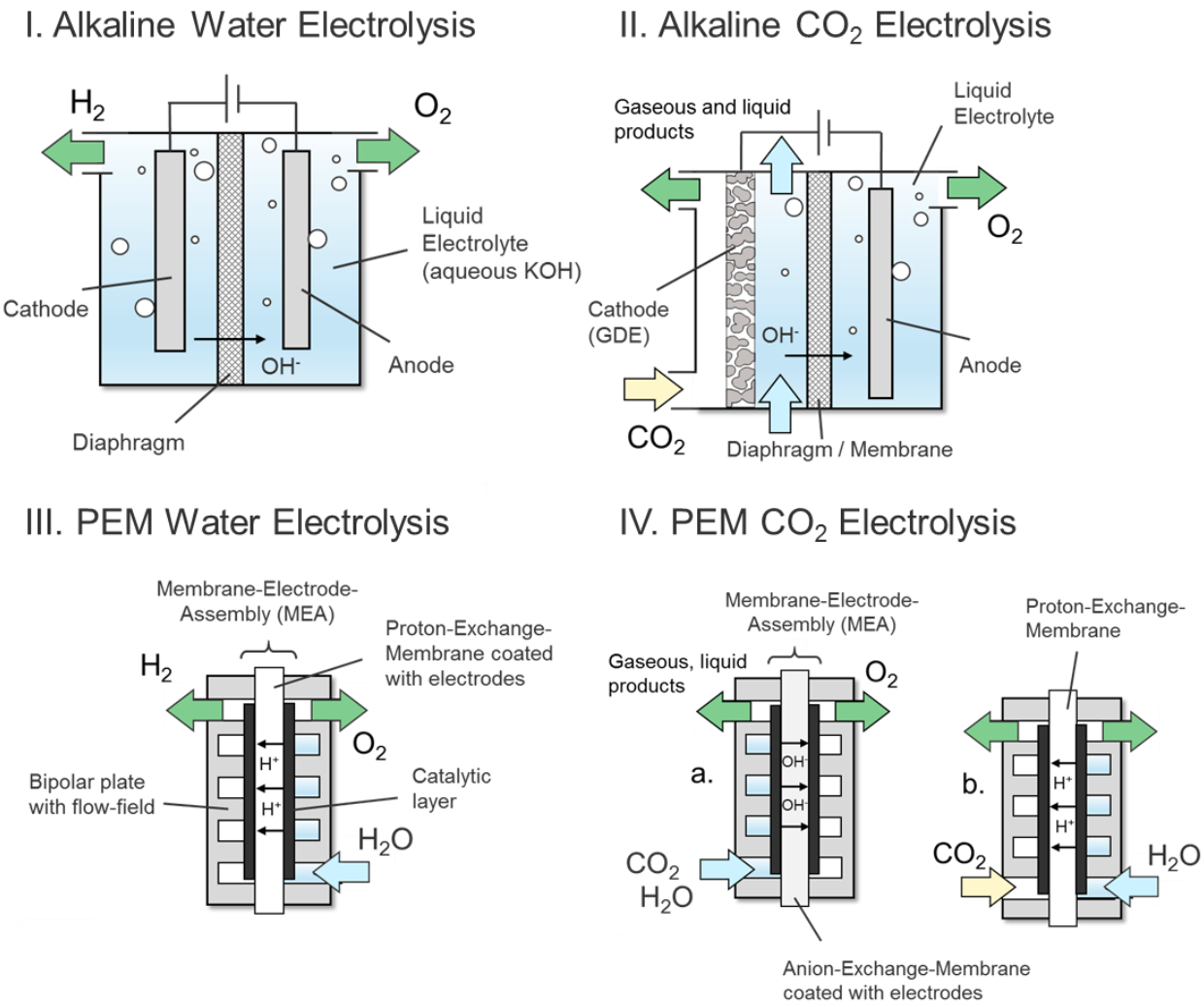

Scheme of considered electrolysis technologies. Alkaline water (I) and CO_2 (II) electrolysis, the latter with gas-diffusion electrode and liquid buffer layer on the cathode side. Polymer-electrolyte membrane (PEM) water electrolysis with proton-exchange membrane (III) and PEM CO_2 electrolysis with anion-exchange membrane (IV, left) and proton-exchange membrane (IV, right)

Making quantitative sense of electromicrobial production

Supplementary Table 1

Summary of assumptions and references that went into analysis model.

	unit	Sc.1	base	Sc.2	PEMEL	References
Investment cost (system, 2030)	€/kW	800	585	370	760	[1]
Conversion factor P/A	kW/m²	7	7	7	32	calc. from [2]
Stack share on investment cost	%	50	50	50	60	[1]
Installation factor	-	1.1	1.1	1.1	1.1	
Installed stack cost per area	€/m²	~3,100	~2,300	~1,400	~16,000	calc.
Maintenance	%	5	5	5	5	[1]
Financial model						
Run time per year	h/year	5000	5000	5000	5000	[3]
Interest rate	%	5	5	5	5	[4]
Loan term	years	20	20	20	20	[4]
Stack cost incl. financial model	€/m²h	0.050	0.037	0.023	0.257	calc.
Electrochemistry					base	
Standard cell voltage	V	1.00	1.23	1.50	585	base: H_2 gen.
Faradaic efficiency	%	90	90	90	7	
Electricity					50	
Electricity price	€/kWh	0.03	0.05	0.07	1.1	[5]

References

1. *Commercialisation of Energy Storage in Europe: Final Report*. (2015).
2. Buttler, A. & Spliethoff, H. Current status of water electrolysis for energy storage, grid balancing and sector coupling via power-to-gas and power-to-liquids: A review. *Renew. Sustain. Energy Rev.* **82,** 2440–2454 (2018).
3. Bazzanella, A. M. & Ausfelder, F. *Low carbon energy and feedstock for the European chemical industry*. (2017).
4. Verma, S., Kim, B., Jhong, H. R. M., Ma, S. & Kenis, P. J. A. A gross-margin model for defining technoeconomic benchmarks in the electroreduction of CO_2. *ChemSusChem* **9,** 1972–1979 (2016).
5. *Quarterly report on European Electricity Markets*. *Market Observatory for Energy* **11,** (2018).